



Title	A wideband 60 GHz class-E/F2 power amplifier in 40nm CMOS
Authors(s)	Babaie, Masoud, Staszewski, Robert Bogdan
Publication date	2015-05-19
Publication information	Babaie, Masoud, and Robert Bogdan Staszewski. "A Wideband 60 GHz Class-E/F2 Power Amplifier in 40nm CMOS." IEEE, 2015.
Conference details	2015 IEEE Radio Frequency Integrated Circuits (RFIC) Symposium, Phoenix, Arizona, USA, 17 - 19 May 2015
Publisher	IEEE
Item record/more information	http://hdl.handle.net/10197/7317
Publisher's statement	© © 2015 IEEE. Personal use of this material is permitted. Permission from IEEE must be obtained for all other uses, in any current or future media, including reprinting/republishing this material for advertising or promotional purposes, creating new collective works, for resale or redistribution to servers or lists, or reuse of any copyrighted component of this work in other works.
Publisher's version (DOI)	10.1109/RFIC.2015.7337743

Downloaded 2023-10-06T13:54:56Z

The UCD community has made this article openly available. Please share how this access benefits you. Your story matters! (@ucd_oa)



© Some rights reserved. For more information

A Wideband 60 GHz Class-E/F₂ Power Amplifier in 40nm CMOS

Masoud Babaie¹, Robert Bogdan Staszewski^{1,2}, Luca Galatro¹, and Marco Spirito¹

¹ Delft University of Technology, The Netherlands

² University College Dublin, Ireland

(email: M.Masoud.Babaie@ieee.org)

Abstract— This paper presents a fully integrated 60 GHz power amplifier in 40 nm CMOS that reaches the highest reported product of power-added efficiency and bandwidth. It is achieved through low/moderate coupling-factor transformers in the preliminary stages and a proper second harmonic termination of the output stage, such that it can operate as a class-E/F₂ switched-mode PA at the saturation point. The three-stage PA delivers 17.9 dBm saturated output power with 20% peak PAE. It demonstrates a bandwidth of 9.7 GHz with a peak gain of 21.6 dB.

Index Terms— Power amplifier, mm-wave, class-E/F₂, switched-mode, transformer, PA stability

I. INTRODUCTION

A key challenge of 60 GHz CMOS radios is a poor efficiency of their power amplifier (PA). Employing nonlinear switched-mode PAs within digitally intensive transmitter architectures, such as outphasing and direct digital-to-RF conversion [1], can improve the total system efficiency. However, switching at mm-wave is not trivial due to the large output capacitance and low current driving capability of CMOS transistors.

In this paper we propose a new architecture of a fully integrated *switched-mode* wideband 60 GHz PA in standard digital 40 nm CMOS. By a proper second-harmonic termination of its output matching network, the required systematic peak current of the final stage is reduced such that it can act as a class-E/F₂ *switched-mode* PA at saturation. Transformers of low/moderate coupling are also utilized in the preliminary stages to improve the overall bandwidth. We also propose a technique to stabilize transformer-based mm-wave amplifiers against various modes of undesired oscillations.

II. BENEFITS AND CONSTRAINTS OF CLASS-E/F PA

It is shown in Kee et al. [2] that drain efficiency η_D of zero-voltage switching (ZVS) PA of Fig. 1 (a) can be written in terms of a set of technology dependent parameters (R_{on} , C_{out}) and a set of matching network or waveform dependent parameters (F_C , F_{PI} , F_I). To better understand the tradeoffs in mm-wave designs, we extend the results of [2] to:

$$\eta_D = 1 - \frac{R_{on} I_{rms}^2}{V_{DD} I_{DC}} = 1 - \left(\frac{I_{rms}}{I_{DC}} \right)^2 \frac{I_{DC}}{C_S \omega_0 (V_{DD} - V_{sat})} \cdot \left(\frac{V_{DD} - V_{sat}}{V_{DD}} \right) \left(\frac{C_S}{C_{out}} \right) (R_{on} C_{out}) \omega_0. \quad (1)$$

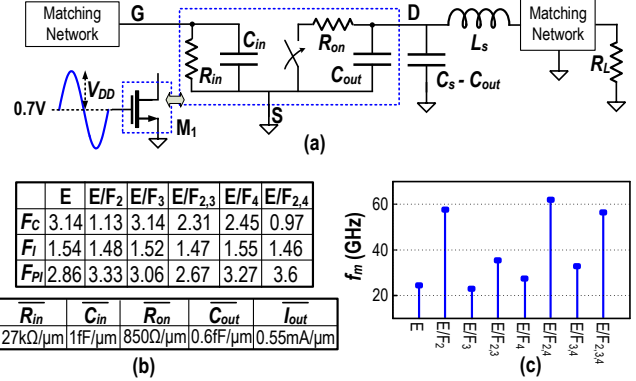


Fig. 1. (a) Class-E/F PA schematic; (b) waveform FoM and technology parameters; (c) maximum operating frequency for different flavors of class-E/F PA in TSMC 40 nm LP CMOS, as predicted from (6).

The waveform FoM's are defined as

$$F_I = \frac{I_{rms}}{I_{DC}}, F_C = \frac{I_{DC}}{C_S \omega_0 (V_{DD} - V_{sat})}, F_{PI} = \frac{I_{peak}}{I_{DC}}. \quad (2)$$

where R_{on} and C_{out} are, respectively, on-state channel resistance and off-state output capacitance of M_1 transistor. Note that $R_{on} \times C_{out}$ is invariant to changes of M_1 's width. I_{DC} and I_{rms} are defined as the average and RMS values of M_1 drain current, and C_S is the PA desired shunt capacitance to satisfy the ZVS criterion. V_{sat} represents the transistor's average V_{DS} in on-state. Note that since F_C should not change over the $\omega_0 = 2\pi f_0$ operating frequency, C_S has to reduce with increasing f_0 . Hence, C_S limits the transistor's width at mm-wave, which leads to a dramatic increase in R_{on} and thus V_{sat} of the switching device. Consequently, we include the effect of V_{sat} in η_D and F_C definitions in (1) and (2) to achieve more practical analytic results than in [2]. V_{sat} can be calculated from

$$P_{Loss} = V_{sat} I_{DC} = R_{on} I_{rms}^2 \rightarrow V_{sat} = R_{on} I_{DC} F_I^2. \quad (3)$$

By replacing $I_{DC} = F_C C_S \omega_0 (V_{DD} - V_{sat})$ in (3),

$$V_{sat} = V_{DD} \frac{F_C F_I^2 R_{on} C_{out} \omega_0}{\alpha + F_C F_I^2 R_{on} C_{out} \omega_0} \quad (4)$$

where $\alpha = C_{out}/C_S$ denotes how much the required C_S for the class-E/F operation is occupied by M_1 's self-capacitance. It is also instructive to go one step further than [2] and calculate the class-E/F PA characteristics

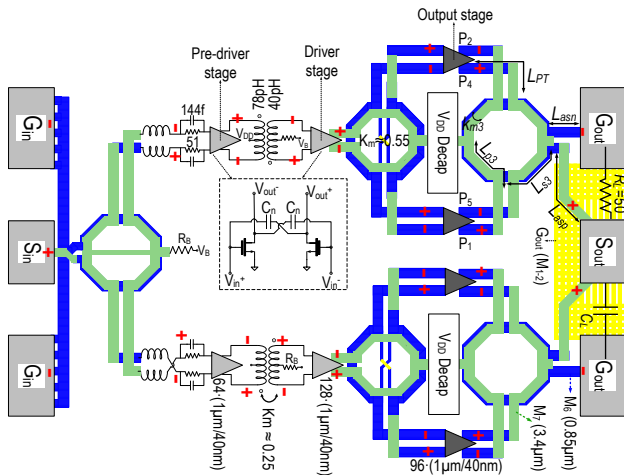


Fig. 2. Schematic and layout of the proposed 60 GHz PA.

based on waveform and technology parameters of Fig. 1(b). MOS devices must satisfy two conditions for the proper switched-mode PA operation. First, transistor cut-off frequency f_{max} should be at least 3-4 \times higher than f_0 . NMOS f_{max} is about 250 GHz in TSMC 40-nm LP CMOS. Hence, the transistors should be fast enough to turn on/off rapidly at $f_0=60$ GHz. Second, the transistor must be capable of providing the required systematic peak current during switching while its output capacitance C_{out} remains below C_S . Consequently,

$$I_{out} = J_{out} \cdot W = \overline{I_{out}} \cdot \frac{C_{out}}{C_{out}} \geq I_{peak} \quad (5)$$

Indeed, MOS transistor current capability (I_{out}/C_{out}) is relatively poor and puts a limit on the maximum operating frequency f_m of switched-mode PAs. By using (3), F_{PI} and F_C definitions in (5), f_m could be derived as

$$f_m = \frac{\alpha \overline{I_{out}}}{2\pi C_{out} F_C (F_{PI} V_{DD} - F_I^2 R_{on} I_{out})}. \quad (6)$$

The f_m increases by migrating to a more advanced technology or by using a matching network with lower F_{PI} and F_C . Figure 1(c) predicts f_m for different flavors of class-E/F PA by utilizing (6) and waveform and technology parameters of Fig. 1(b). Figure 1(c) indicates f_m can be extended to 60 GHz in the 40 nm CMOS for the class-E/F₂ operation when the transistor's effective load is realized as open circuit at the 2nd harmonic, $2\omega_0$.

By substituting (4) in (1), η_D is simplified to

$$\eta_D = \frac{\alpha}{\alpha + F_C F_I^2 R_{on} C_{out} \omega_0}. \quad (7)$$

Eqs.(4) and (7) indicate that V_{sat} and η_D improve by using a matching network with lower F_I and F_C , which is in line with f_m optimization. Eq.(7) also predicts $\eta_D=65\%$ for 40 nm class-E/F₂ PA at 60 GHz. The switch

size is relatively small such that its R_{on} degrades η_D to somewhere between class-A and B. It can be shown that PA's output power and gain can be calculated by

$$P_{out} = \eta_D P_{DC} = \left(\frac{\alpha V_{DD}}{\alpha + F_C F_I^2 R_{on} C_{out} \omega_0} \right)^2 F_C C_S \omega_0, \quad (8)$$

$$G_p = \frac{P_{out}}{V_{DD}^2/2R_{in}} = \frac{2\alpha F_C R_{in} C_{out} \omega_0}{(\alpha + F_C F_I^2 R_{on} C_{out} \omega_0)^2}. \quad (9)$$

Unfortunately, both P_{out} and G_p reduce almost linearly with F_C . Consequently, higher f_m of class-E/F₂ operation is achieved through painful reduction of P_{out} and precious device G_p , which can potentially reduce the total PAE.

III. POWER AMPLIFIER DESIGN

Figure 2 shows the schematic of the proposed PA. A 3-stage common-source pseudo-differential pair is chosen to compensate for the gain penalty G_p of the class-E/F₂ operation in the last stage. A transformer-based power splitter converts the singled-ended S_{in} input to two differential signals feeding pre-drivers. Another set of splitters is added before the four parallel units of the output stage. A combination of series-parallel combining is used in the output matching network. A 2-way differential series combining is achieved by a distributed active transformer [3] to reduce the resistive load seen by each transistor such that the systematic P_{out} reduction of class-E/F₂ is partially compensated. By exploiting parallel combining, the output devices can be smaller for the same P_{out} , which effectively improves the transistors' internal loss and f_{max} . Hence, they can generate a stronger 2nd harmonic current which is beneficial for the class-E/F₂ operation.

Figure 3(a) shows the half-circuit model of the output matching network. The total effective inductance at the output of the matching network $(4L_{s3}+L_{asn}+L_{asp})/2$ must resonate with the parasitic capacitance of the pad (C_L) to optimize its insertion loss. Furthermore, the combination of the transformer leakage inductance $L_{p3}(1-k_{m3}^2)$ and the effective inductance of differential strip-lines L_{PT} along C_S must satisfy zero-voltage and zero-slope class-E switching criteria by [2]

$$(L_{p3}(1-k_{m3}^2) + L_{PT}) C_S = 1/4.74\omega_0^2. \quad (10)$$

The matching network behavior is entirely different for the common-mode (CM) input signals. The transformer's coupling factor is negligible in CM excitation and thus R_L , C_L and L_{s3} cannot be seen by the even harmonics. Hence, the transmission line and transformer primary inductance, which is seen by CM signals, has to resonate with C_S at $2\omega_0$ to satisfy the class-E/F₂ operation. Figure 3(c) indicates F_C is just slightly degraded when CM resonance lies 25% away from $2\omega_0$. Thus, this PA is quite insensitive to the precise CM inductance value, which promotes a wide bandwidth operation.

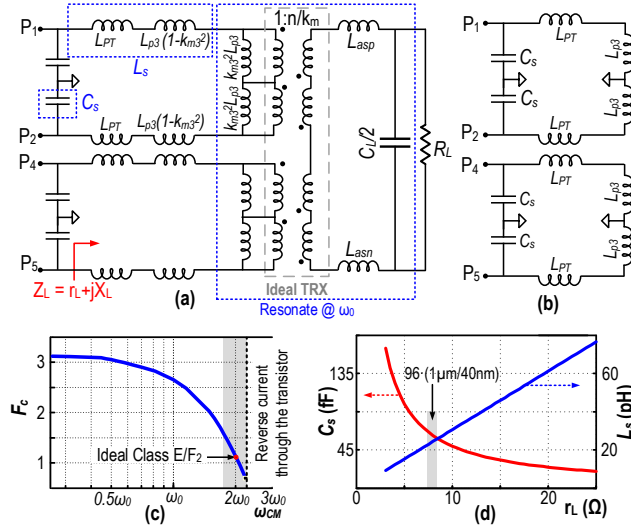


Fig. 3. Equivalent half-circuit model of output matching network for (a) DM, and (b) CM excitations; (c) F_C versus CM resonant frequency; (d) required L_S and C_S for class-E/F operation versus resistive load seen by switch transistor.

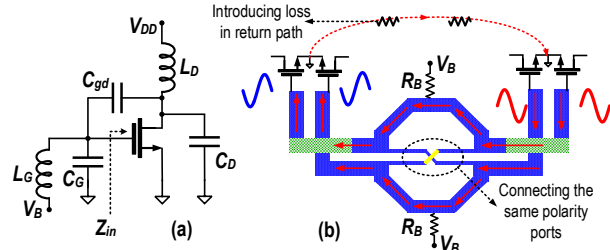


Fig. 4. (a) Half-circuit of PA pseudo-differential stage, (b) damping the undesired combination of CM and DM oscillation.

Figure 3(d) shows the optimum required class-E/F₂ PA shunt capacitance C_S and series inductance L_S at fundamental frequency versus the load resistance presented by the matching network. The matching network geometry design is initiated by choosing the switch transistor dimension such that its output capacitor absorbs the entire C_S . However, C_S also depends on L_S and the load resistance presented by the matching network, as can be gathered from Fig. 3(d). Hence, several iterations are needed to find the optimal size combination of the transistor, transformer and matching network. This procedure results in an optimal unit power transistor size of $96(1\mu\text{m}/40\text{nm})$ with 1.3 dB insertion loss of the output matching network. Note that the class-E/F₂ optimal combination is different from the goal of maximizing the output power or gain.

Each pseudo-differential pair along with their parasitic capacitance C_{gd} and matching networks (see Fig. 4(a)) can potentially act as two coupled Pierce oscillators and create CM instability. It can be shown that its resonant frequency is very close to the operating frequency ($\approx 0.7\text{--}0.8\omega_0$) such

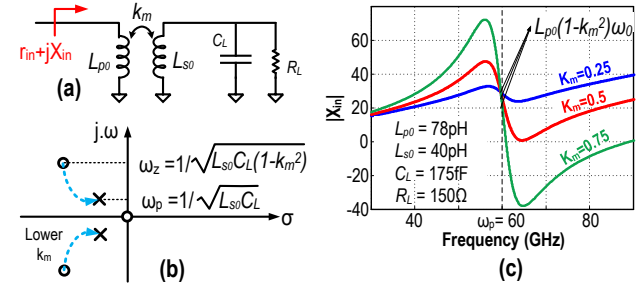


Fig. 5. (a) Transformer for inter-stage matching, (b) poles and zeros of X_{in} , (c) $|X_{in}|$ versus frequency for different k_m .

that neither adding an RC stabilization network at the MOS gate nor matching network loss can dampen the oscillation without affecting the precious power gain at ω_0 . Fortunately, using relatively large resistors ($R_B \sim 3\text{ k}\Omega$) between the center tap of the secondary windings of the input and inter-stage transformers and gate bias voltage can cancel out the CM currents at the transformer secondary winding. Hence, any CM oscillation will be dampened. Nevertheless, a combination of CM and differential-mode (DM) oscillation can potentially happen in the transformer splitter. As shown in Fig. 4(b), each differential pair could oscillate in CM but with 180° phase shift to each other. Hence, neither neutralization capacitors nor R_B will damp this oscillation. We propose adding a weak cross connection between the splitter's in-phase ports to reduce the loop gain in this oscillation mode without affecting the splitter's main function. Another solution would be to add a lossy path between the ground connections of two pseudo-differential pairs across the splitter.

The effective Q-factor of the PA input/output matching network is degraded by the $50\ \Omega$ load and RF pad parasitic capacitance, $C_L \leq 50\ \text{fF}$, to about 1–2 at 60 GHz, thus making these networks wideband. However, the input impedance of MOS transistors is considered as load to the inter-stage matching network, where $Q_{eff} = \overline{R_{in} C_{in} \omega_0} \approx 10$ at 60 GHz. Hence, the impedance seen at the input of the transformer network ($r_{in} + jX_{in}$ in Fig. 5(a)) changes significantly over frequency and thus limits the PA BW. Figure 5(b) depicts the position of zeros and poles of the X_{in} transfer function. Under a high k_m case (≥ 0.7), the conjugate zeros pair occurs at much higher frequency than the poles of the system. Hence, a large variation is seen in X_{in} (see Fig. 5(c)). However, the zero/pole pairs come closer together with lower k_m and a flatter region is observed in the X_{in} plot. Hence, the transistor sees its desired impedance over a wider frequency range. The additional insertion loss penalty is only $\leq 1.5\ \text{dB}$ over the BW by using a $k_m = 0.25$ transformer. That penalty happens at the primary stages where it has negligible effect on the total PAE [4].

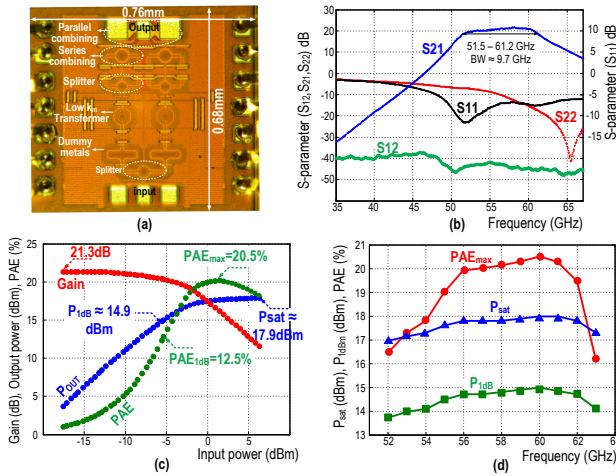


Fig. 6. (a) Chip micrograph; (b) measured S-parameters; (c) large-signal measurement at 60 GHz; (d) PA characteristics versus frequency.

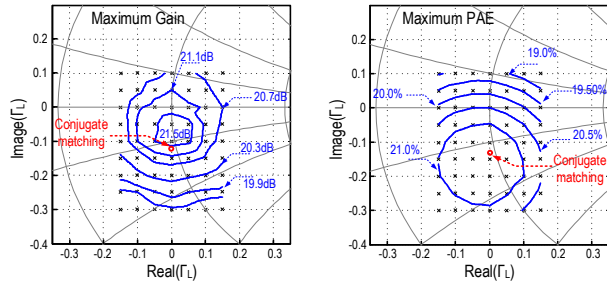


Fig. 7. Measured constant maximum gain and PAE contours.

TABLE I
COMPARISON TABLE OF 60 GHz CMOS POWER AMPLIFIERS

	This work	[6]	[1]	[3]	[4]
Technology	40nm LP	40nm LP	65nm GP	65nm GP	28nm LP
V_{DD}	1V	1V	1V	1V	2.1V
Gain(dB)	21.5	17	N/A	20.3	24.4
BW_{-3dB}	9.7GHz	5.5GHz	7GHz	9GHz	11GHz
P_{-1dB} (dBm)	14.9	13.8	N/A	15	11.7
P_{sat} (dBm)	17.9	17	9.6	18.6	16.5
PAE_{max}	20.5%	30.3%	28.5%	15.1%	12.6%
Area (mm ²)	0.25	0.115	0.11	0.175	0.22
$PAE/BW/f_0$	3.32%	2.78%	3.32%	2.27%	2.31%

IV. MEASUREMENT RESULTS

The proposed mm-wave PA is fabricated in a standard digital TSMC 40 nm 1.1V 1P7M LP CMOS technology. The chip micrograph is shown in Fig.6(a). The transformers are completely filled with dummy metal strips to comply with the strict metal density rules. The amount of the metal fills right underneath the transformer windings is kept at minimum to reduce the extra parasitic capacitance and eddy current losses. However, EM simulations reveal an additional loss of 0.2–0.4 dB for each matching network. The measured

S-parameters are shown in Fig. 6(b). With 1 V supply, the PA achieves a peak power gain of 21.6 dB at 58 GHz with BW_{-3dB} of 9.7 GHz (51.5 to 61.2 GHz). The S_{11} , S_{22} and S_{12} are respectively better than -6, -7 and -42 dB within 50–67 GHz. The large-signal measurements are done by a mixed-signal active load-pull setup [5]. Consuming ≤ 0.3 A from a 1 V supply, the measured P_{1dB} and P_{sat} are respectively 14.9 dBm and 17.9 dBm with 20.5% PAE_{max} at 60 GHz. The power performance is characterized in Fig. 6(d). The following parameters are maintained over 52–63 GHz: 16.9 dBm P_{sat} , 13.8 dBm P_{1dB} , and 16% PAE. Figure 7 illustrates PA's constant gain and PAE contours and also verifies the PA stability over load variation.

Table I shows a comparison of state-of-the-art 60 GHz CMOS PAs. Our PA achieves comparable BW_{-3dB} as in a 28 nm PA [4], but with a much higher PAE. For $P_{sat} \approx 18$ dBm, only class-AB PA in [6] shows better PAE, but at a lower gain and BW. Furthermore, the product of PAE and BW reaches the best reported.

V. CONCLUSION

The benefits, constraints and trade-offs of different flavors of class-E/F PAs have been investigated from the mm-wave viewpoint. The resulting new proposed architecture of a fully integrated 60 GHz power amplifier was realized in 40-nm bulk CMOS. This PA utilizes a proper second-harmonic termination in the last stage and low/moderate magnetic coupling factor transformers in the intermediate stages to reach the best product of PAE and BW. The PA is also stabilized against the combination of DM and CM oscillation mode.

ACKNOWLEDGMENT

The authors thank Prof. Ali M. Niknejad for technical discussions and reviewing this paper, TSMC for chip fabrication, Integrand Software for EMX license, and European ERC Grant 307624 for financial support.

REFERENCES

- [1] J. Chen, *et al.*, "A digitally modulated mm-wave cartesian beamforming transmitter with quadrature spatial combining," *ISSCC*, Feb. 2013, pp. 232–233.
- [2] S. Kee, *et al.*, "The class-E/F family of switching amplifiers," *IEEE Trans. Microwave Theory Tech.*, vol. 51, no. 6, pp. 1677–1690, June 2003.
- [3] J. Chen, *et al.*, "A compact 1V 18.6dBm 60GHz power amplifier in 65nm CMOS," *ISSCC*, Feb. 2011, pp. 423–433.
- [4] S. Thyagarajan, *et al.*, "A 60GHz drain-source neutralized wideband linear power amplifier in 28nm CMOS," *IEEE TCAS-I*, vol. 61, no. 8, pp. 2253–2262, Aug. 2014.
- [5] L. Galatro, *et al.*, "60GHz mixed signal active load pull for millimeter wave devices characterization," *80th ARFTG Symp. Dig.*, Nov. 2012, pp. 1–6.
- [6] D. Zhao, *et al.*, "A 60-GHz dual-mode class AB power amplifier in 40-nm CMOS" *IEEE Journal of Solid-State Circuits*, vol. 48, no. 10, pp. 2323–2337, Oct. 2013.